

## Bandgap Fluorescence of Carbon Nanotubes Observed

Members of the fullerene family of materials have been the subject of intense research due to their novel physical and chemical properties. Optical studies of carbon nanotubes have been hampered by the tendency of these materials to aggregate into bundles. Richard Smalley, R. Bruce Weisman, and their co-workers in the Department of Chemistry at Rice University have reported a separation methodology that produced aqueous suspensions of single nanotubes encased in a nonperturbing layer of sodium dodecyl sulfate (SDS) surfactant, allowing the optical properties of single nanotubes to be studied (see figure). These isolated single-walled carbon nanotubes were found to exhibit structured absorption and photoluminescence (PL) in the near-IR region. Both the absorbance and PL were affected by reversible protonation of the nanotubes in solution. According to Smalley, "optical activity in the near-IR [spectrum] implies potential applications in the fiberoptic communications and bio-imaging technologies."

The synthesis and purification of the individual nanotubes were described in the July 26 issue of *Science*. The researchers synthesized the nanotubes in a high-pressure CO reactor. The raw nanotube product was sonicated in an aqueous dispersion of SDS to break up the nanotube bundles. The single nanotubes were then separated from the remaining bundles by centrifugation and dispersed in deuterium oxide for spectroscopic studies. Atomic force microscopy showed that the sonicated nanotubes varied in length from 80 nm to 200 nm with an average length of 130 nm, an expected distribution for heavily sonicated nanotubes. The absence of damage to the nanotube walls was confirmed by Raman spectroscopy.

The absorption spectra of the isolated single nanotubes showed spectral structure that was enhanced and blueshifted compared with those of nanotube bundles. The nanotubes were also found to display bright, structured photoluminescence with a quantum yield of 0.1%. The PL peaks closely matched the absorbance peaks, indicating that the PL comes from the nanotubes. It was found that protonation of the nanotube side walls at pH <5 resulted in the broadening of absorption spectral structure and the loss of PL. Absorption spectral structure and PL intensity were restored following removal of the adsorbed species by adjusting the pH to >7, or irradiating the suspension with UV light to induce photo-

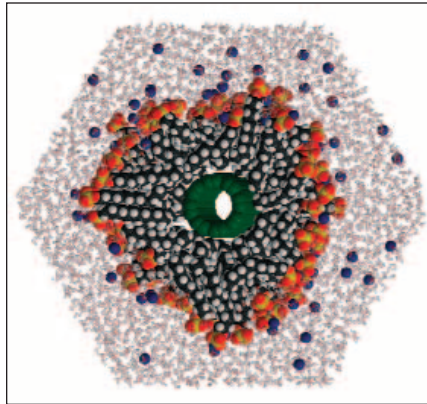


Figure. Molecular dynamics simulation of a single nanotube encased in a micelle of sodium dodecyl sulfate in water. Such nanotubes were found to exhibit photoluminescence at near-IR wavelengths.

desorption. As part of a continuing effort to understand fullerene-based materials, the Smalley and Weisman groups are currently investigating the electronic structure of isolated single-walled nanotubes through detailed spectroscopic analysis.

GREG KHITROV

## Alternative Fabrication Process for Nanostructured Alloys Promises Dramatic Cost Reduction

The improvement in mechanical properties achieved by materials with ultra-fine-sized grains represents an advantage for many advanced applications. One of the typical properties of these materials is superplasticity: Although superplasticity is observed at half of the melting temperature in materials with micrometer-sized grains, it is observed at lower temperatures in materials with nanometer-sized grains. Fabrication of these materials is usually accomplished using vapor-phase condensation, high-energy ball milling, or severe plastic deformation. The first two methods are used mainly to produce fine powders and the last to produce bulk material. However, these processes are costly, and plastic deformation in particular is still in development for large-scale production. An alternative fabrication method has now been proposed by a group of scientists from Purdue University in a rapid communication in the October issue of the *Journal of Materials Research*. It is based on the large shear strains experienced by a material forming chips during machining, which makes the chips nanocrystalline. In order to demonstrate this, the scientists performed electron microscopy observations

in chips from a wide range of metals and alloys: oxygen-free high-conductivity (OFHC) copper, iron, low-carbon steel (1018), stainless steel (316L), martensite steel (AISI 52100), and nickel.

The shear plane formed between the machining tool and the surface of the bulk material defines the area where deformation occurs. The machining parameters chosen by the researchers minimized the increase in temperature in the shear plane in all cases. Chips thus produced were 100–3000  $\mu\text{m}$  wide, 100–1000  $\mu\text{m}$  thick, and no less than 5 mm long. Observations in the transmission electron microscope (TEM) of OFHC copper samples showed elongated grains with an average width of  $175 \pm 100$  nm and an average length of  $685 \pm 190$  nm. All grains had sizes of <1000 nm. Observations also revealed a high density of dislocations and both small- and large-angle grain boundaries. These features are characteristic of severely deformed nanocrystalline microstructures. Chips made from iron and different types of steel also showed similar microstructures.

Hardness values of the chips show significant increases compared with those of the bulk materials—150% in stainless steel, 200% in OFHC copper and iron, and 225% in nickel—typical for nanocrystalline microstructures. Chip hardness values rose to levels comparable to those of the similar nanocrystalline materials obtained using traditional fabrication methods. Furthermore, after conducting a special "quick-stop" test, the researchers were able to measure the increase in hardness in an OFHC copper chip while it was still attached to the bulk material. The researchers detected a sudden increase in Vickers hardness across the shear plane section, from 57 kg/mm<sup>2</sup> in the bulk to 150 kg/mm<sup>2</sup> in the chip. At the magnification where bulk grains were resolved using TEM, the researchers were not able to observe any grain structure in the attached chip.

The researchers also demonstrated that the cost involved in fabricating nanocrystalline chips from machining bulk materials is of the order of a few dollars per pound on top of the cost of the bulk material, which represents a tremendous reduction from traditional processes that can cost more than \$100 per pound. Bulk materials could be synthesized from chips thus obtained by means of powder metallurgy, ball attrition, or jet milling. Different methods to fabricate metal-matrix and polymer-matrix composites could also take advantage of these inexpensive nanocrystalline chips.

SIARI S. SOSA

### Dye-DNA-Lipid Thin Films Exhibit Durable Amplified Spontaneous Emission

A considerable obstacle in the current development of solid-state lasers is durability. Researchers at the Chitose Institute of Science and Technology, Japan, have demonstrated that thin films composed of DNA, lipid, and a hemicyanine dye have the potential for a practical, durable, solid-state laser.

As reported in the August 19 issue of *Applied Physics Letters*, Y. Kawabe and co-workers fabricated thin films by casting on Teflon plates a dichloromethane-methanol solution containing DNA-hexadecyltrimethylammonium (HTMA) and 4-[4-(dimethylamino) styryl]-1-dococylpyridinium bromide (DMASDPB), a derivatized hemicyanine dye known for its nonlinear optical properties. Self-standing films were formed by evaporating the solvent in vacuum. Film thickness was controlled by varying the concentration. Fluorescence enhancement of DMASDPB in DNA was previously confirmed.

Threshold-energy levels were determined by measuring the light intensity emitted from the samples as a function of pump-pulse energy. The output of a frequency-doubled Nd<sup>3+</sup>:YAG laser ( $\lambda = 532$  nm,  $\tau_p = 7$  ns), used as the pump source, was focused with a normal incident angle onto a 1 mm  $\times$  5 mm stripe on the sample. The emitted light was observed perpendicular to the incident beam along the direction of the stripe.

Emission peaked at 631 nm under low-intensity pumping. A shift in the emission peak to 624 nm with concomitant spectral narrowing were observed under high-intensity pumping. While output energy is proportional to pump energy in the low-intensity region, superlinear dependence is evident for energies greater than 0.5 mJ/cm<sup>2</sup>. The researchers attribute the spectral narrowing to amplification because the narrowing and superlinear enhancement occur at the same intensity. Amplification occurs at relatively low self-absorption. In addition, the emitted light is linearly polarized parallel to the film surface, indicating enhanced amplification. The researchers conclude from these results that amplified spontaneous emission occurs in the DMASDPB-HTMA films.

The role played by DNA was investigated in two control experiments. First, thin films were fabricated with poly(methyl methacrylate) and DMASDPB. The resulting films showed strong fluorescence under the same pumping conditions, but neither intensity enhancement nor spectral narrowing was observed. In the second control experiment, a simple laser cavity

containing a chloroform solution of DMASDPB was prepared. No indication of lasing was observed. The same apparatus confirmed lasing for some conventional laser dyes as well as for a chloroform solution of DMASDPB and HTMA. The researchers believe that this clearly demonstrates that DMASDPB acquires the ability to lase through its interaction with DNA, which likely alters the dye's electronic state. Further structural and spectroscopic studies to investigate the details of the dye-DNA interaction are planned by the researchers.

In this preliminary study, which was performed in air at room temperature, a reduction in lasing performance of only a few percent was observed after two hours of operation; the total fluence of energy during the test was 210 J/cm<sup>2</sup>. The researchers believe that the low threshold, good performance, and long durability exhibited by their DMASDPB-HTMA films demonstrate their potential for practical use as solid-state lasers, especially because their method can be applied to chromophores other than conventional laser dyes.

STEVEN TROHALAKI

### DNA-Templated Nanowire Fabrication Technique Developed

As the feature sizes of electronic circuits approach the limits of optical lithography, the costs of traditional micro- and nanolithography techniques used in the electronics industry will become unacceptably high. Recently, several groups have studied approaches using DNA for nanowiring. However, due to the relatively poor intrinsic electric conductivity of DNA, metallization is necessary. In search of new fabrication technologies, a research group from Sony International (Europe) GmbH reported in the September issue of *Nano Letters* on their technique for metallizing DNA using negatively charged tris(hydroxymethyl)phosphine-capped gold nanoparticles (THP-AuNPs).

An aqueous colloidal sol of THP-AuNPs was synthesized by mixing HAuCl<sub>4</sub> solution and hydrolyzed tetrakis(hydroxymethyl)phosphonium chloride solution. The resultant particles were characterized by lithium-ion exchange, inductively coupled plasma-atomic emission spectroscopy analysis, and gel electrophoresis. The results showed that the particles were negatively charged with an average individual net charge of approximately 15 *e*.

Two steps are involved in metallization: formation of conjugates between DNA and metal nanoparticles (NPs) and enlargement of the NPs by electroless plating. In the first step, *in situ* or *ex situ*

# Find what you need in 5 minutes or less



You'll find more than 40,000 different items in our online Catalog, the majority in stock and ready for shipment.

Need something special? We can help with that, too. Take a moment now and see how **Goodfellow can help.**

**Web: [www.goodfellow.com](http://www.goodfellow.com)**  
 (Secure, online ordering)  
**Real live person: 1-800-821-2870**  
**E-mail: [info@goodfellow.com](mailto:info@goodfellow.com)**  
**Fax: 1-800-283-2020**

**Goodfellow**  
 METALS & MATERIALS  
 FOR RESEARCH & INDUSTRY

© 2002 Goodfellow Corporation

Circle No. 14 on Inside Back Cover

approaches are used, based on the formation of the metal NPs in the DNA-NP conjugate. In this research, the *ex situ* method was employed because the researchers discovered that negatively charged THP-AuNPs can bind densely to the negatively charged calf thymus DNA. During the metallization procedure, DNA was first immobilized on a silicon substrate by O<sub>2</sub> plasma treatment to enhance immobilization and spin-coating to elongate the molecules. Before the THP-AuNP sol was applied to the substrate, the particles were precipitated in ethanol, then dissolved in an ethanol-water solution. Optimum results with respect to density of particle templating, avoidance of excess particles on the substrate, and lack of defects in the resultant wires were obtained at an ethanol:water ratio of 95:5. After rinsing and drying, the samples were treated with an electroless gold plating solution in order to form conductive nanowires for further characterization.

Atomic force microscopy revealed that after calf thymus DNA molecules on a silicon substrate were treated with THP-AuNPs in 95% ethanol, the DNA molecules were decorated with particles, with some excess particles (0.7 nm to 2 nm in size) also on the substrate. Scanning electron microscopy images showed that the electroless gold plating of the resulting DNA-AuNP conjugates provides nanowires ~30–40 nm in width and longer than 2 μm. The good contrast against the silicon surface indicates high conductivity and the metallization was restricted almost entirely to the DNA. The results of the electrical transport capabilities of the DNA nanowires showed that their electrical conductivities were about one-thousandth that of bulk gold.

To determine what kind of mechanism controls the binding between THP-AuNPs and DNA, several hypotheses were considered, based on the interactions between THP-AuNPs and DNA, such as adsorption of THP-AuNPs to hydrophilic DNA molecules on the silicon oxide surface, hydrogen-bonding interactions in between, ligand replacement by groups on DNA that can coordinate to the AuNP surface, and the covalent bonding between THP and amino groups of the DNA base.

The process can be finished in ~10 min, but the *in situ* approaches that employ metal salts or complexes as precursors take longer than 1 h. The technique reported here by O. Harnack and co-workers could be used for future electronic circuits because it can lower the fabrication cost and is suitable for feature sizes below the current limit of optical lithography. However, issues about the binding mechanism between the

THP-AuNPs and DNA, and how the solvent and substrate influence the process, need to be further studied.

YUE HU

### Direct Ink-Jet Printing Assembles ZrO<sub>2</sub> Powder into 3D Shape

Three-dimensional shapes can be created from ceramic powders by forcing droplets of “ink” containing the powder through an ink-jet nozzle, layering the deposition to generate height. Xinglong Zhao and colleagues from the University of London in conjunction with Jin-Hua Song from Brunel University report their work on the creation of vertical walls from ceramic materials using ink-jet printing in the August issue of the *Journal of the American Ceramic Society*. Zhao and colleagues have created mazes (replicas of one at Hampton Court Palace outside London) with various wall-thickness values where the smallest gap between walls was  $170 \pm 10 \mu\text{m}$ . This technique has applications in rapid prototyping and the creation of ceramic molds, circuit boards, and biosensors.

A ZrO<sub>2</sub> powder with an average particle size of 0.45 μm was mixed with a commercial dispersant to create a mixture with an estimated ZrO<sub>2</sub> powder volume fraction of 0.63. The combination was then stirred with an ultrasonic probe for 5 min and milled for approximately 30 min to disperse the powder into the liquid and break down the agglomerates. The ink-jet print head contained 500 50-μm nozzles with a print width of 70 mm and a computer-controlled sliding table. The table print speed was 500 mm/s and registered its position at the edge of the track between passes to ensure accuracy in the *y* printing direction. To assure uniformity, the ink was filtered through a 5-μm mesh, and the air was removed from the system by repeated extraction and insertion of the ink through the print head until no signs

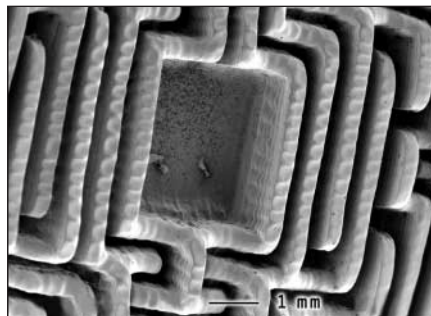


Figure. Scanning electron micrograph of vertical ceramic walls created by direct ceramic ink-jet printing.

of bubbles appeared in the tubing. Between passes, a hot-air blower was used for 20 s to enhance the drying procedure and reduce spreading. Since the ink remained opaque after 10 h, the final samples were allowed to dry for 24 h before pyrolyzation and sintering.

The results of this process based on a maze pattern can be seen in the figure. Although individual droplets cannot be seen, an overall surface texture results in part from coalescence during the drying process. Very straight vertical walls were achieved, although the height was not uniform due to a wall-thickness effect, where thinner walls had reduced height, and also because of in-filling of the center parts of the maze. The researchers said that complications resulting from ink drying and spreading will need to be considered during the scaling-up process.

CHRISTINE RUSSELL

### Simulations Show a Hexatic Phase in Porous Media

In the Kosterlitz–Thouless–Halperin–Nelson–Young (KTHNY) theory, when a two-dimensional crystal melts, it first becomes hexatic by the unbinding of dislocation pairs, and then becomes liquid through the unbinding of disclination pairs. However, early simulations did not exhibit the hexatic phase. Now, researchers at the Massachusetts Institute of Technology, North Carolina State University, and Adam Mickiewicz University in Poland have observed the hexatic phase, consistent with the theory, in molecular simulations of simple fluids in narrow slit-shaped carbon pores. The stability of the phase increased with the strength of the fluid–wall interaction. Experimental measurements confirmed the existence of the hexatic phase.

In Monte Carlo simulations of large systems of the order of 64,000 molecules, the crystalline–hexatic and hexatic–liquid transitions were observed for simple fluids of spherical molecules. R. Radhakrishnan of MIT and co-workers reported in the August 12 issue of *Physical Review Letters* that they modeled the fluid–fluid interaction of CCl<sub>4</sub> with a Lennard–Jones potential and the fluid–wall interaction with a 10-4-3 Steele potential.

The simulated pores were of two different widths, 0.911 nm or 1.41 nm, and contained either one or two layers of adsorbed CCl<sub>4</sub>. The researchers monitored the in-plane positional and orientational correlation functions to determine the nature of the confined phase.

For the two-layer system, at 360 K the positional correlation function was isotropic, and the orientational one showed

exponential decay, representing a liquid phase. At 330 K, the positional correlation function remained isotropic but the orientational one showed algebraic decay, a signature of the hexatic phase. At 290 K, the system became a two-dimensional hexagonal crystal, showing quasi-long-range positional order and long-range orientational order. The scaling of the correlation functions was consistent with KTHNY theory.

The melting transition was second order when the pores contained one layer of molecules and became weakly first order for pores containing two layers. The researchers attribute the change to interaction between defect configurations in the two layers.

Differential scanning calorimetry (DSC) measurements of  $\text{CCl}_4$  and aniline in an activated carbon fiber with slit-shaped pores narrowly distributed around a mean size of 1.4 nm showed peaks near temperatures predicted in the simulations. Nonlinear dielectric effect (NDE) signals diverged with a scaling consistent with the theory.

Dielectric relaxation spectroscopy (DRS) of adsorbed aniline, a dipolar fluid, showed sharp changes, indicating phase transitions near the predicted temperatures. The orientational relaxation times of the adsorbed molecules were typical of a hexatic phase between 298 K and 324 K. Below that range, the time scales were typical of a crystal, and above it, they were typical of a liquid.

ELIZABETH A. SHACK

### Direct Observation of Intercalated Cs in Zeolite $\text{Si}_{32}\text{O}_{64}$ Yields Example of Inorganic Electride

Understanding the properties of nanoscale arrays of metal atoms may allow scientists to manipulate these properties to produce nanomagnets, nanocatalysts, nanodevices, and composites with better optical properties than are currently possible. However, such applications require a detailed knowledge of the materials' atomic-level structure. Thomas Vogt, a physicist at Brookhaven National Laboratory, and scientists from Michigan State University led by physicist Valeri Petkov (now at Central Michigan University), have demonstrated that the atomic pair distribution function (PDF) technique allows them to decipher such fine-level nanostructures.

Their analysis of a material composed of cesium ions trapped inside nano-sized pores of the silicon oxide zeolite  $\text{Si}_{32}\text{O}_{64}$  is described in the August 12 issue of *Physical Review Letters*. This material is also the first example of a room-temperature inorganic "electride," a stable separation

of positively charged cations and electrons with properties determined by the topology of the pores in the host matrix.

In traditional crystallography, long-range order and symmetry, specifically the repeating three-dimensional (3D) patterns in the crystals, give rise to sharp Bragg peaks in the x-ray powder diffraction pattern, which are then used to determine the atomic structures. Materials constructed at the nanoscale, however, lack this long-range order and often accommodate a large number of defects and local disorder. The result, said Petkov, is that the diffraction patterns of nanocrystals are much more diffuse with few, if any, Bragg peaks.

To overcome this problem, the team of scientists employed the PDF technique, a nontraditional experimental approach, to read between the Bragg peaks of data produced by traditional x-ray powder diffraction experiments. With the PDF technique, the scientists revealed direct structural evidence that cesium is intercalated in the nano-sized pores of the silicon oxide zeolite in the form of positively charged cesium ions arranged in short-range-order

zigzag chains. This verifies that  $\text{Cs}_x\text{Si}_{32}\text{O}_{64}$  is a room-temperature stable inorganic electride, the scientists said.

"Electrides are novel materials that are just beginning to be studied," said Petkov. First results show that they could be used as reducing materials in chemical synthesis of other materials and that they have useful electronic properties such as low-energy electron emission.

### Carbon-Nanotube Transistor Arrays Used for Fabrication of Multistage Complementary Logic Devices and Ring Oscillators

Carbon nanotubes are expected to be the most promising candidates for building blocks for the next generation of electronic devices, predominantly due to low surface scattering and nanoscale channel widths. A group of researchers at the Department of Chemistry and the Laboratory for Advanced Materials at Stanford University have demonstrated a fabrication route for multistage complementary NOR, OR, NAND, and AND logic gates and ring oscillators based on arrays of *p*- and *n*-type

C O O L U N D E R P R E S S U R E

## Hall Measurement System

MMR's low cost, Turnkey Hall Effect Measurement System provides user programmed computer controlled measurement and data acquisition over a temperature range of -200°C to +300°C – without the use of liquid nitrogen. The system measures magneto resistivity, four point resistivity, sheet resistivity, sheet number, mobility, Hall coefficient, and carrier density using the Van der Pauw and Hall measurement techniques.

Measurement Ranges (somewhat dependent on sample thickness)	
Resistivity	10 <sup>-4</sup> Ohm-cm to 10 <sup>+13</sup> Ohm-cm
Carrier Mobility	1cm <sup>2</sup> / volt-sec to 10 <sup>+7</sup> cm <sup>2</sup> / volt-sec
Carrier Density	10 <sup>+3</sup> cm <sup>-3</sup> to 10 <sup>+19</sup> cm <sup>-3</sup>

For more information about the Hall Effect Measurement System, contact Bob Paugh at 650 / 962-9620 or bobp@mmr.com. Or visit our web page at <http://www.mmr.com>.

MMR Technologies, Inc.

Circle No. 12 on Inside Back Cover

nanotube field-effect transistors (FETs). Their main approach involved converting *p*-type FETs in an array into *n*-type FETs by a local electrical manipulation under a vacuum.

As reported in the September issue of *Nano Letters*, Ali Javey, Hongjie Dai, and co-workers performed the fabrication of the *p*-type transistor device depositing single-wall nanotubes (SWNTs) between metal electrodes formed on the photolithographically patterned SiO<sub>2</sub> layer. Device fabrication involves the synthesis of SWNT arrays by chemical vapor deposition of methane on substrates pre-patterned with catalyst and bottom-*W*-gate arrays. Thus-obtained 4 × 4 mm<sup>2</sup> chips contain about 100 devices. The yield of the acceptable SWNT FETs was found to be in the range of 20–30%. The researchers achieved a *p*-type FET conversion into *n*-type by applying a high local gate voltage (–40 V) combined with a large source-drain (20 V) bias for a certain duration under vacuum (10<sup>–8</sup> Torr). The yield of this technique results in ~50% *p*–*n* conversion. The researchers suggested a mechanism for this conversion based on reversible desorption of molecular oxygen from SWNTs, leading to significant *n*-channel conduction. The ability of local manipulation of SWNT FETs into *n*-type has enabled the researchers to obtain multiple *n*-FETs and *p*-FETs on a SWNT chip and construct complementary logic devices and ring oscillators.

The researchers concluded that simple computing operations are possible by using the high percentage of semiconducting SWNTs and the ability for local gating, manipulation, and doping of individual SWNT FETs.

ANDREI A. ELISEEV

### AFM Enables Study of Biomolecules' Interaction with Minerals

Treavor Kendall, a graduate student in the mineral-microbe group in the Department of Geological Sciences at the Virginia Polytechnic Institute and State University, has demonstrated the use of an atomic force microscope (AFM) to study how biomolecules extract minerals. At the 12th Annual V.M. Goldschmidt Conference, an international geochemistry conference held August 18–23 in Davos, Switzerland, Kendall described his experiments on how the bacteria *Azotobacter vinelandii* acquire iron.

Kendall said that the bacteria release the organic molecules siderophores, which have an affinity for iron. While studies have shown how siderophores

interact with iron in water, Kendall's research explored how they acquire iron that is embedded in a mineral structure.

"This is important," said Kendall, "because minerals are a primary source of iron in the environment." He specifically looked at the affinity between azotobactin and the mineral goethite, an important iron oxide in soils worldwide, he said.

The research team covalently attached the molecule to the AFM tip using a common protein-coupling technique. The activated tip was then used to probe various minerals including goethite and diaspore, goethite's isostructural aluminum equivalent. The sensitivity of the AFM allowed the forces of interaction associated with the azotobactin and each mineral surface to be measured. A two- to threefold increase in the adhesion forces between the siderophore molecule and the iron-containing mineral over the forces measured for the aluminum-containing mineral was observed. According to the researchers, this large adhesion force between the siderophore and goethite could be attenuated upon the addition of small amounts of soluble iron, indicating the interaction captured in this measurement was specific between the azotobactin chelating groups and the iron in the surface. These force measurements demonstrating azotobactin's strong specific affinity for iron in a solid form suggests azotobactin may be directly coordinating with iron in the mineral surface groups, they said. Such a coordination could destabilize the Fe–O bonds in the mineral, driving dissolution and subsequent iron release.

This is a unique result, said Kendall, because larger siderophores such as azotobactin are often believed to acquire iron by acting as scavengers; that is, they steal iron from other, smaller, lower-affinity ligands in solution without interacting with the mineral surface. On the contrary, these results indicate that direct surface contact is a distinct possibility.

According to Kendall, siderophores are used in medicine to treat people who have too much iron in their blood. The siderophore locks up the iron so it is no longer toxic. The ability to measure iron affinity at the molecular level may allow researchers to refine siderophore medicinal use and detect iron concentrations in very small amounts by using them as a chemosensor.

### Gradient Structures of Nanoparticles Prepared on Chemical Template

Scientists from North Carolina State University (NCSU) and the National Institute of Standards and Technology (NIST) have

created a material with a gradient of gold nanoparticles on a silica-covered silicon surface using a molecular template. The material provides evidence that nanoparticles can form a gradient of decreasing concentration along a surface. A description of the material appears in the July 23 issue of *Langmuir*.

"This material promises to be the first in a series with many applications in electronics, chemistry, and the life sciences," said Rajendra Bhat, a graduate student from NCSU and the lead author of the study. Bhat worked with Jan Genzer, a chemical engineering professor at NCSU, and Daniel Fischer, a physicist from NIST.

To build the material, the scientists first prepared a ~1-nm-thick layer of amine-terminated organosilanes on a rectangular surface of silicon (4.5 cm × 1.2 cm) with a 2-nm-thick native SiO<sub>x</sub> layer. The head glues to the surface, while the amine-terminated tail sticks out, acting like a hook waiting for a gold nanoparticle to attach to it, said Genzer, leader of the NCSU team. The organosilane molecules, emitted vertically in the form of a vapor by a source close to one side of the surface, slowly fell on the surface with decreasing concentration as the distance from the source increased, thus creating a number-density gradient to serve as a molecular template.

The next step was to dip the material in a colloidal solution containing the gold nanoparticles. In the solution, the amine-terminated tails of the organosilane mole-

### Corrections

Ihab F. El-Kady's name was omitted from a news article about a 3D photonic metallic crystal reported in the July 2002 issue of *MRS Bulletin*, page 488. El-Kady served as the lead of the research team from the Ames Laboratory at Iowa State University.

Brian D. Madsen's name was misspelled in the July 2002 issue of *MRS Bulletin*, page 490. He is part of the research team at Northwestern University who contributed to research on solid-oxide fuel cells, enabling hydrocarbon oxidation without coking.

A presentation at the Advanced Metallization Conference 2001 was reported incorrectly in the February 2002 issue of *MRS Bulletin*, page 138. The correct attribution is as follows: The last session of AMC2001 addressed atomic layer deposition (ALD), including an invited paper by K.E. Elers (ASM Microchemistry).

cles took on a positive charge, so that the negatively charged gold particles attached to the oppositely charged tails underneath.

To visualize the gradient of gold particles, Bhat and his colleagues used an atomic force microscope, and to look at the gradient of the organosilane molecules, the scientists used near-edge x-ray absorption fine structure (NEXAFS) spectroscopy.

"We needed to confirm that both the gold particles and the sticky groups followed the same underlying gradient template," Bhat said. "The results from both techniques were expected to coincide if the particles were attaching to the underlying layer of sticky molecules. Our results show exactly that."

According to Genzer, the distinguishing feature of this approach is that the particles follow a pre-designed chemical template provided by the organosilane sticky groups. "The ability to manipulate the underlying template allows us to prepare gradient structures of nanoparticles with varying characteristics," he said.

The main advantage of the gradient structure, the scientists said, is that large numbers of structures can be combined on a single substrate and used for high-throughput processing. It might, for example, save time for chemists testing clusters of nanoparticles used as catalysts.

Fischer said, "Clusters made of different numbers of nanoparticles could be put on a single surface, and scientists

could test this surface only once in a chemical reaction, instead of having to run each cluster separately through the reaction." The material could also be used as a sensor to detect species that have specific affinities for nanoparticles, or as a filter to select particles of given sizes. □

FOR MORE RESEARCH NEWS ON MATERIALS SCIENCE . . .

. . . access the Materials Research Society Web site:

[www.mrs.org/gateway/matl\\_news.html](http://www.mrs.org/gateway/matl_news.html)

CHEMICAL-MECHANICAL POLISHING

**Don't Miss These Symposium Proceedings on CMP from the Materials Research Society**

**Chemical-Mechanical Polishing 2001—Advances and Future Challenges\***

Volume 671-B  
\$69.00 MRS Member  
\$79.00 U.S. List  
\$91.00 Non-U.S.

**Chemical-Mechanical Polishing 2000—Fundamentals and Materials Issues\***

Volume 613-B  
\$38.00 MRS Member  
\$48.00 U.S. List  
\$59.00 Non-U.S.

**Chemical-Mechanical Polishing—Fundamentals and Challenges**

Volume 566-B  
\$60.00 MRS Member  
\$70.00 U.S. List  
\$77.00 Non-U.S.

\* This volume is also available in electronic format on the MRS Web site, with FREE access for all current MRS members.

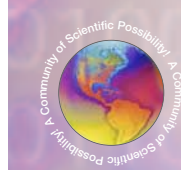
For more information, or to order any of the proceedings volumes listed above, contact the MRS Customer Services Department.



Tel 724-779-3003  
Fax 724-779-8313  
Email info@mrs.org

[www.mrs.org/publications/books/](http://www.mrs.org/publications/books/)

MRS Membership Directory



Now Online

[www.mrs.org/members/directory](http://www.mrs.org/members/directory)



Stop!

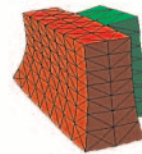
Don't buy a different software product for every modeling problem.

With FlexPDE you can solve whole families of 2D and 3D field problems!

Like electromagnetics, heatflow, deformation, and lots more. Steady-state, time-dependent, time-harmonic or eigenvalues.



Open Tube Combustion Reactor



3D Multi-material Thermoelasticity



T-Septate Waveguide

With a redesigned user interface, FlexPDE 3.0 is more than ever the indispensable tool for scientists and engineers • FlexPDE 3.0 is a scripted finite element model builder for partial differential equations systems • Linear or Nonlinear • 2D or 3D plus time or eigenvalues • Unlimited number of variables • Windows, Unix, Linux or Mac OSX • Download a demo from our website

**PDE Solutions Inc**

P.O. Box 4217 • Antioch, CA • 94531  
925-776-2407 • FAX 925-776-2406  
[www.pdesolutions.com](http://www.pdesolutions.com)

Circle No. 10 on Inside Back Cover